Research Article

Journal of Physical Organic Chemistry

Received: 14 May 2011, Accepted: 20 May 2011, Published online in Wiley Online Library: 2011

(wileyonlinelibrary.com) DOI: 10.1002/poc.1901

Investigation of cation–anion interaction in 1-(2-hydroxyethyl)-3-methylimidazolium-based ion pairs by density functional theory calculations and experiments

Shiguo Zhang[a], Xiujuan Qi[a], Xiangyuan Ma[a], Liujin Lu[a], Qinghua Zhang[a] and Youquan Deng[a]*

Gas-phase structure, hydrogen bonding, and cation–anion interactions of a series of 1-(2-hydroxyethyl)-3-methylimidazolium ($[HOEMIm]^+$)-based ionic liquids (hereafter called hydroxyl ILs) with different anions (X=$[NTf_2]^-$, $[PF_6]^-$, $[ClO_4]^-$, $[BF_4]^-$, $[DCA]^-$, $[NO_3]^-$, $[AC]^-$ and $[Cl]^-$), as well as 1-ethyl-3-methylimizolium ($[EMIm]^+$)-based ionic liquids (hereafter called nonhydroxyl ILs), were investigated by density functional theory calculations and experiments. Electrostatic potential surfaces and optimized structures of isolated ions, and ion pairs of all ILs have been obtained through calculations at the Becke, three-parameter, Lee–Yang–Parr/6-31+G(d,p) level and their hydrogen bonding behavior was further studied by the polarity and Kamlet–Taft Parameters, and ^{1}H-NMR analysis. In $[EMIm]^+$-based nonhydroxyl ILs, hydrogen bonding preferred to be formed between anions and C2–H on the imidazolium ring, while in $[HOEMIm]^+$-based hydroxyl ILs, it was replaced by a much stronger one that preferably formed between anions and OH. The O–H···X hydrogen bonding is much more anion-dependent than the C2–H···X, and it is weakened when the anion is changed from $[AC]^-$ to $[NTf_2]^-$. The different interaction between $[HOEMIm]^+$ and variable anion involving O–H···X hydrogen bonding resulted in significant effect on their bulk phase properties such as ^{1}H-NMR shift, polarity and hydrogen-bond donor ability (acidity, α). Copyright © 2011 John Wiley & Sons, Ltd.
Supporting information may be found in the online version of this article.

Keywords: calculation; cation–anion interaction; hydrogen bonding; hydroxyl; ionic liquids; polarity

INTRODUCTION

Ionic liquids (ILs), typically composed of organic cations and inorganic/organic anions, have attracted considerable attention in various areas such as organic synthesis, catalysis, electrochemical devices, and solvent extraction because of their attractive properties, which are not available in molecular solvents.[1–8] Increasing interest in ILs has been recently aroused because of their novel applications in chemical sensors,[9] dye-sensitized solar cells,[10] energetic materials,[11] lubricants,[12] and electrowetting media,[13] which makes them not just replacement solvents but new platforms for advanced multipurpose materials.

Differing significantly from conventional polar molecular solvents, ILs are single-component systems in which the cations and anions may possibly play independent roles in determining liquid behavior.[14] ILs exhibit interesting solvation and coordination properties that depend on the nature of cations and anions, and the intermolecular interaction between ions. Thus, controlling the interactions between cations and anions will be important in the rational design of ILs.[15] Hydrogen bonding in ILs has been extensively studied because it plays an important role in cation–anion and solvent–solute interactions, as revealed by both experimental and theoretical investigations.[16–20] For example, the hydrogen bond characteristics of ILs was said to be vitally important to design ILs as potential solvents for cellulose.[21]

On the other hand, hydroxyl ILs render classical ILs with useful polarity/solvation properties that have now attracted considerable interest because they can replace traditional volatile alcohols in certain applications such as organic reactions[22,23] and nanomaterial synthesis.[24–27] $[HOEMIm][NTf_2]$ ($[HOEMIm]^+$=1-(2-hydroxyethyl)-3-methylimidazolium) was found to possess higher polarity than $[EMIm]^+$-based ($[EMIm]^+$=1-ethyl-3-methylimidazolium) nonhydroxyl ILs and a much higher *endo/exo* ratio of Diels–Alder reactions produced in the process.[23] Spiropyran exhibited negative photochromism in $[HOEMIm][NTf_2]$ and $[HOEMIm][PF_6]$,[28,29] unlike the positive photochromism it exhibited in general in nonhydroxyl ILs and other hydroxyl ILs such as $[HOEMIm][NO_3]$. One interesting point is that the physicochemical properties and the solvent–solute interactions of hydroxyl ILs are more significantly influenced by the counteranion than nonhydroxyl ILs. More recently, during our research on the solvation and micropolarity in ILs, we found

* *Correspondence to: Y. Deng, Center for Green Chemistry and Catalysis, Lanzhou Institute of Chemical Physics, Chinese Academy of Sciences, Lanzhou, 730000, China. E-mail: ydeng@licp.cas.cn*

a *S. Zhang, X. Qi, X. Ma, L. Lu, Q. Zhang, Y. Deng*
Center for Green Chemistry and Catalysis, Lanzhou Institute of Chemical Physics, Chinese Academy of Sciences, Lanzhou, 730000, China

that $[HOEMIm]^+$-based hydroxyl ILs exhibited anion-dependent polarity, while their corresponding nonhydroxyl ILs exhibited comparable polarity, as indicated by solvatochromic dyes.[30] The preliminary result suggested that the greatly expanded polarity of hydroxyl ILs was correlated to the ionic hydrogen-bonded complexes between the anions and the hydroxyl group on cations.

In the present work, the structure, hydrogen bond, and cation–anion interaction of $[HOEMIm]^+$-based hydroxyl ILs (Fig. 1) with different anions ($[PF_6]^-$, $[NTf_2]^-$, $[ClO_4]^-$, $[DCA]^-$, $[NO_3]^-$, $[Cl]^-$, and $[AC]^-$) were investigated by density functional theory (DFT) calculation combined with experiments to provide a deeper understanding of the effect of the hydroxyl group on the interaction between imidazolium cations and anions, and the subsequent impact on their physicochemical properties.

EXPERIMENTAL

Chemicals and synthesis

All chemicals were commercially available and used as received. 2,6-Diphenyl-4-(2,4,6-triphenyl-*N*-pyridino) phenolate (Reichardt's dye 30), and 2,6-dichloro-4-(2,4,6-triphenyl-*N*-pyridino)phenolate (Reichardt's dye 33) were purchased from Aldrich (Sigma-Aldrich Corp., St. Louis, Missouri, USA). 4-Nitroaniline (98%) and *N*,*N*-dimethyl-4-nitroaniline (>98%) were purchased from Alfa Aesar (Alfa Aesar Corp., Ward Hill, Massachusetts, USA). The syntheses and characterization of all ILs with different cation and anion structures (Fig. 1), namely, 1-ethyl-3-methylimidazolium bis(trifluoromethanesulfonyl)amide ($[EMIm][NTf_2]$), 1-ethyl-3-methylimidazolium hexafluorophosphate ($[EMIm][PF_6]$), 1-ethyl-3-methylimidazolium perchlorate ($[EMIm][ClO_4]$), 1-ethyl-3-methylimidazolium tetrafluoroborate ($[EMIm][BF_4]$), 1-ethyl-3-methylimidazolium dicyanamide ([EMIm][DCA]), 1-ethyl-3-methylimidazolium nitrate ($[EMIm][NO_3]$), 1-ethyl-3-methylimidazolium acetate ([EMIm][AC]), and their corresponding hydroxyl ILs, that is, 1-(2-hydroxyethyl)-3-methylimidazolium bis(trifluoromethanesulfonyl)amide ($[HOEMIm][NTf_2]$), 1-(2-hydroxyethyl)-3-methylimidazolium hexafluorophosphate ($[HOEMIm][PF_6]$), 1-(2-hydroxyethyl)-3-methylimidazolium perchlorate ($[HOEMIm][ClO_4]$), 1-(2-hydroxyethyl)-3-methylimidazolium tetrafluoroborate ($[HOEMIm][BF_4]$), 1-(2-hydroxyethyl)-3-methylimidazolium dicyanamide ([HOEMIm][DCA]), 1-(2-hydroxyethyl)-3-methylimidazolium ($[HOEMIm][NO_3]$), 1-(2-hydroxyethyl)-3-methylimidazolium acetate ([HOEMIm][AC]), and 1-(2-hydroxyethyl)-3-methylimidazolium chloride ([HOEMIm][Cl]) were reported in a previous work.[30]

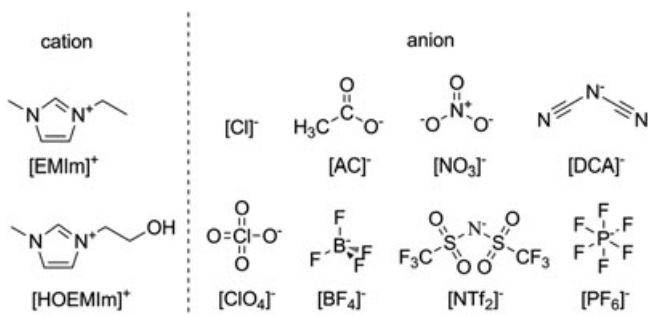

Figure 1. Structures and abbreviations of the cations and anions of ILs used in this study

Determination of $E_T(30)$ and Kamlet–Taft parameters

Polarity and Kamlet–Taft parameters of all ILs were determined by using the solvatochromic probes, that is, Reichardt's dye 30, *N*,*N*-dimethyl-4-nitroaniline, and 4-nitroaniline, according to detailed procedures reported in a previous work.[30]

^{1}H-NMR measurement

^{1}H-NMR spectra were conducted on a Bruker AMX FT (Bruker AXS Inc., Madison, Wisconsin, USA) 400-MHz NMR spectrometer and chemical shifts were reported downfield in parts per million (ppm, δ) from a tetramethylsilane reference. All ILs were dissolved in DMSO-d_6 with the same concentration of 0.2 M for comparison.

Computational analysis (density functional theory calculations)

Density functional theory calculations were performed with the GAUSSIAN 03 (Gaussian, Inc., Wallingford, Connecticut, USA) suite of programs.[31] Geometry optimizations were conducted using the Becke, three-parameter, Lee–Yang–Parr (B3LYP)/6-31+G(d,p) method without any constraint. Frequency calculations were carried out at the same level of theory to confirm that the geometries of ILs were local minima without any imaginary frequency. The energy of the ion-pair formation (ΔE) was estimated using Eqn 1, according to Turner *et al.*[32]

$$\Delta E(\text{kcal/mol}) = 627.5[E_{AX}(\text{au}) - (E_{A+}(\text{au}) + E_{X-}(\text{au}))] \quad (1)$$

where ΔE is the energy of the ion-pair formation and E_{AX}, E_{A+}, E_{X-} are the energy of ionic pair, the isolated cation, and anion, respectively.

The interaction energies were corrected by the basis set superposition errors (BSSE) correction with the counterpoise procedure method advanced by Boys and Bernardi[33] at B3LYP/+G(d,p) level. Zero-point energy (ZPE) correction calculated using the unscaled B3LYP/6-31+G(d,p) frequencies was also taken into account for the calculated interaction energies.

The gas-phase acidity considered in this study was calculated as the free energy change of the following reaction in the gas phase at 298 K, 1 atm, according to the established method.[34]

$$A - H(g) \rightarrow A^-(g) + H^+(g) \quad (2)$$

RESULTS AND DISCUSSION

Structure of $[HOEMIm]^+$

The most stable conformations of $[EMIm]^+$ and $[HOEMIm]^+$ are given in Fig. 2 (their selected parameters are given in Table S1). The optimized geometry of $[EMIm]^+$ is in good agreement with previous results.[19,35] Obviously, the bond lengths of C2–H, C4–H, and C5–H are almost equal to each other, and the imidazolium ring exhibits a coplanar structure. When an OH substituted the terminated hydrogen on the ethyl group, although the bond angle and bond length of methyl, ethyl, and imidazolium is less influenced, the dihedral angle of C2–N1–C13–C15 is changed from −73.9° to −114.2°. The fact that the negative oxygen is close to C2–H was probably caused by the intramolecular hydrogen bonding between OH and C2–H6.

Considering that the electrostatic potential surfaces (ESP) has been found to be an effective tool for analyzing and predicting

Journal of Physical Organic Chemistry

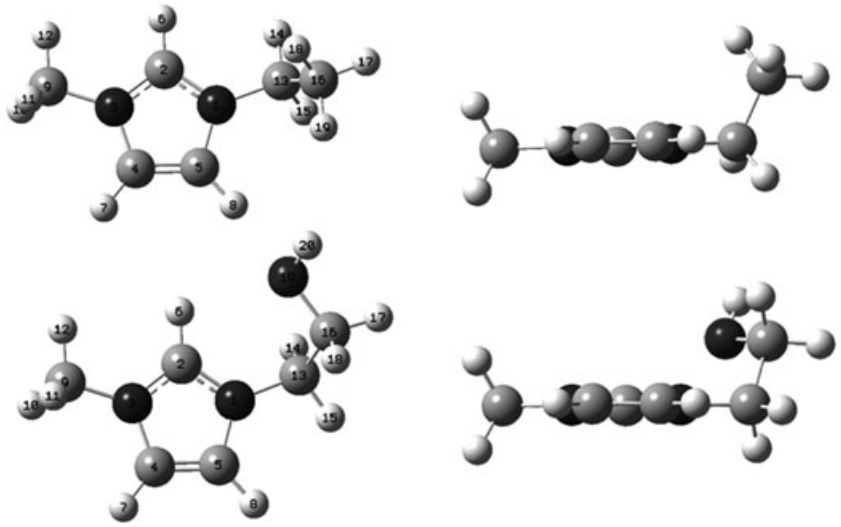

Figure 2. Optimized geometries of isolated cations $[EMIm]^+$ and $[HOEMIm]^+$

noncovalent interactions,[35–37] the ESP for $[EMIm]^+$, $[HOEMIm]^+$, and all anions (X) were constructed to qualitatively gain the possible interaction modes between cations and anions. As can be seen in Fig. 3, the high positively charged region in the $[EMIm]^+$ cation is around the C2–H group followed by the regions around the C4/C5–H atoms attached to the imidazolium ring and the other H atoms in the side chains, which is in good agreement with previous results.[35,38] However, in $[HOEMIm]^+$, the ESP strongly suggests that the hydrogen atom at the OH group is more positive than those in the imidazolium ring, and the positive charge decreases in the order O–H > C2–H > C4/C5–H. This indicates that the presence of the OH in the imidazolium cation makes it a better hydrogen bond donor than C2–H. The negative regions of all anions are always on the electronegative atom such as N, O, and F. For example, the highest negatively charged region in the $[NTf_2]^-$ anion appears on the central nitrogen atom.

As expected, the formation of ILs between the $[HOEMIm]^+$-based cation and variable anion should occur in those regions possessing more positive charges and more negative charges.[39] [HOEMIm][AC] is given as an example for a detailed interpretation of optimization of hydroxyl ILs. The favorable sites (more negative charges) for proton attack in $[AC]^-$ are concentrated on the regions around both carbonyl and oxygen atoms. Both

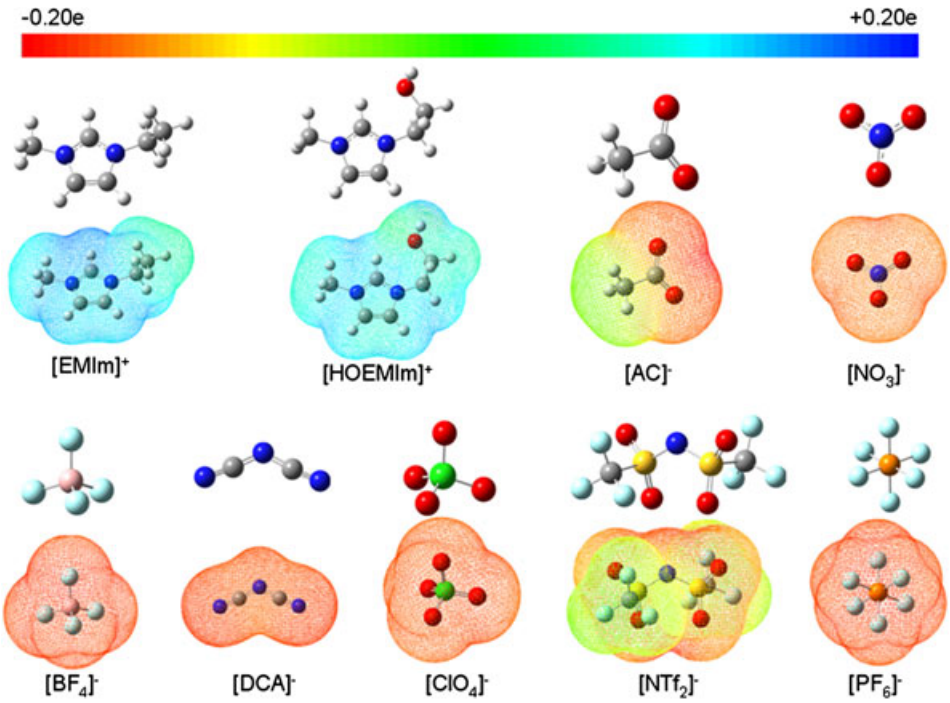

Figure 3. Optimized geometries of the isolated cations and anions (the corresponding electrostatic potential surfaces for them are presented below, where the red and blue indicate regions of more negative and positive charges, respectively, and the isodensity contours are 0.0004 electron/bohr)

the ESP of $[HOEMIm]^+$ and $[AC]^-$ revealed that seven principal conformations are possible for [HOEMIm][Ac], that is, hydrogen bonding formed between $[AC]^-$ and (**A**)-H7, H8, (**B**)-H14, H20, (**C**)-H7, H11, (**D**)-H8, H15, (**E**)-H6, H20, (**F**)-H6, H14, and (**G**)-H6, H12 (labels of atoms are indicated in Fig. 2), as illustrated in Fig. 4. However, during the optimization process, the last three preliminary configurations, that is, **E**, **F**, and **G**, have all been collapsed into the same geometry, complex (**E**). Thus, only five representative complexes (**A–E**) have been optimized. The structural parameters of the five complexes are listed in Table 1.

As clearly seen in Fig. 4, the optimized structures for **A–E** are organized by cation–anion interaction through two hydrogen

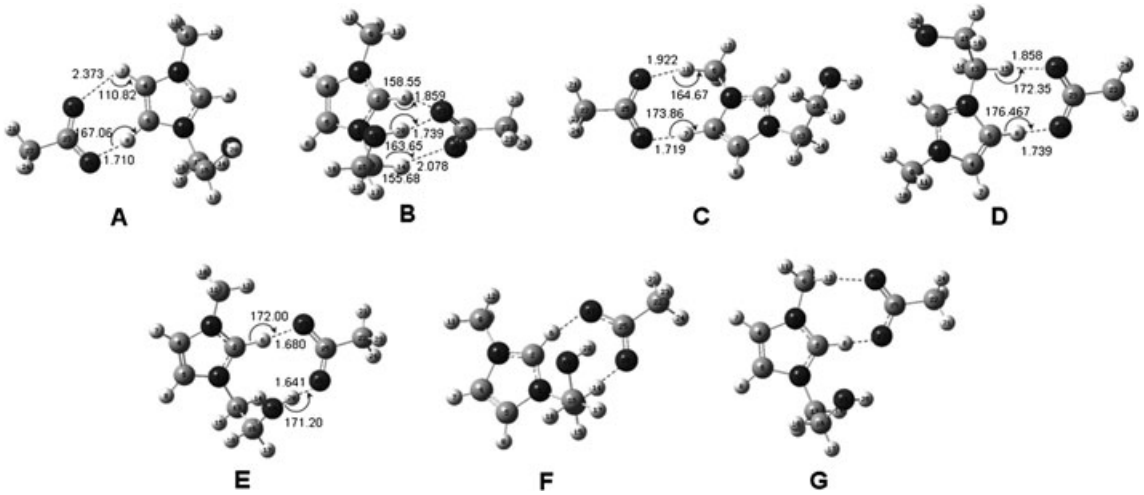

Figure 4. The optimized conformations (**A–E**) of [HOEMIm][AC] ion pairs (the principal conformations of **F** and **G** were also given for illustration)

Table 1. Bond lengths (Å), bond angles (deg), dihedral angles (D, deg), and interaction energies (ΔE_c, kcal/mol) of five [HOEMIm][AC] ion-pairs (**A–E** in Figure 4)

	A	B	C	D	E	$[EMIm]^+$	$[HOEMIm]^+$
N1–C2	1.342	1.338	1.347	1.340	1.340	1.339	1.342
C2–N3	1.342	1.342	1.336	1.342	1.342	1.340	1.339
N3–C4	1.388	1.387	1.385	1.388	1.386	1.383	1.384
C4–C5	1.365	1.364	1.367	1.367	1.364	1.365	1.364
C5–N1	1.386	1.382	1.390	1.387	1.385	1.383	1.384
C2–H6	1.078	1.102	1.078	1.079	1.124	1.079	1.079
C4–H7	1.080	1.078	1.121	1.078	1.078	1.079	1.079
C5–H8	1.121	1.078	1.078	1.118	1.078	1.079	1.079
N1–C13	1.467	1.474	1.468	1.481	1.471	1.484	1.479
N3–C9	1.461	1.462	1.473	1.461	1.464	1.471	1.471
C9–H12	1.091	1.090	1.091	1.090	1.091	1.090	1.090
C13–H14	1.093	1.098	1.096	1.096	1.092	1.092	1.093
O19–H20	0.965	0.994	0.966	0.966	1.005	—	0.966
θ(N1–C2–N3)	108.0	108.2	108.4	108.4	107.8	109.0	108.7
θ(N3–C4–C5)	107.5	106.7	105.9	107.8	106.6	107.1	107.0
θ(N1–C13–C16)	112.1	111.4	113.2	112.4	111.0	112.4	112.4
θ(C13–C16–O19)	107.4	113.5	112.5	113.8	112.2	—	107.0
θ(C16–O19–H20)	109.6	111.2	109.9	109.0	108.4	—	110.4
D(N1–C2–N3–C4)	0.4	0.2	−0.2	−0.2	0.8	0.0	0.0
D(C2–N3–C4–C5)	−0.2	0.1	−0.1	0.1	−0.2	0.0	0.0
D(C2–N1–C13–C16)	82.7	75.7	46.8	42.4	82.4	—	65.4
D(N1–C13–C16–O19)	−66.0	−48.9	−67.4	−65. 7	−52.0	—	−62.4
D(C13–C16–O19–H20)	171.6	−50.9	−88.7	−84.4	−59.2	—	−173.8
ΔE (kcal/mol)	−85.7	−101.7	−86.5	−89.9	−105.2	—	—
ΔE_{ZPE} (kcal/mol)	0.3	1.4	0.5	0.5	1.1	—	—
ΔE_{BSSE} (kcal/mol)	0.6	1.1	0.7	0.8	1.1	—	—
ΔE_C (kcal/mol)[a]	−84.8	−99.2	−85.3	−88.6	−103.0		

[a] $\Delta E_c = \Delta E + \Delta E_{ZPE} + \Delta E_{BSSE}$ at the B3LYP/6-31+G(d,p) level, where ΔE is the energy of the ion-pair formation; ΔE_{ZPE} is the energy difference in theZPE correction; ΔE_{BSSE} is the energy difference in the basis set superposition error.

bonds between the acidic hydrogen on the cation and the oxygen on the anion. The gas-phase acidity of OH in [HOEMIm][AC] (**E**), calculated by a previously reported method[34] is 354.5 kcal/mol. The resulting hydrogen bonding is nearly a line with angles of O–H···X close to 180° and bond lengths much shorter than the van der Waals distance.[40] Small energy differences were obtained between the five conformers (**A, C, D**, and **B, E**), thus ZPEs and BSSEs may alter which is the most stable conformer. As shown in Table 1, both ZPE and BSSE for the ion pairs are only on the order of 1 kcal/mol, and also vary only slightly between conformers. These corrections and the final energy differences are also documented in Table 1. For the five complexes, the interaction energies with ZPE and BSSE correction range from −84.8 to −103.0 kcal/mol (Table 1), where (**E**) is more stable than the others by about 3.6–18.2 kcal/mol. This is consistent with the results of ESP where the most possible interaction sites of $[HOEMIm]^+$ with $[AC]^-$ occurred on O–H and C2–H.

Structure of [HOEMIm][X]

With the optimization procedure of [HOEMIm][AC] in mind, structures of the other hydroxyl ILs with various anions (X = $[NTf_2]^-$, $[PF_6]^-$, $[ClO_4]^-$, $[BF_4]^-$, $[DCA]^-$, $[NO_3]^-$, and $[Cl]^-$) were optimized and the most stable geometries are shown in Fig. 6, together with the comparable result for nonhydroxyl ILs (Fig. 5). For all nonhydroxyl ILs, the anions were located in front of the imidazolium ring, where the atoms of more negative charges are close to the methyl, ethyl, and in particular, C2–H (Fig. 5). In detail, $[PF_6]^-$, $[ClO_4]^-$ and $[BF_4]^-$ are above the imidazolium ring, while $[Cl]^-$, $[AC]^-$, $[NO_3]^-$, and $[DCA]^-$, are nearly located in the plane of the imidazolium ring and generally much closer to the methyl group. In contrast, $[NTf_2]^-$ located its S–N–S core in the plane of the imidazolium ring with each CF_3 group above or below the plane. The dihedral angle of C2–N1–C13–C16 in imidazolium is anion-dependent and changed from 45.64° ([EMIm][Cl]) to

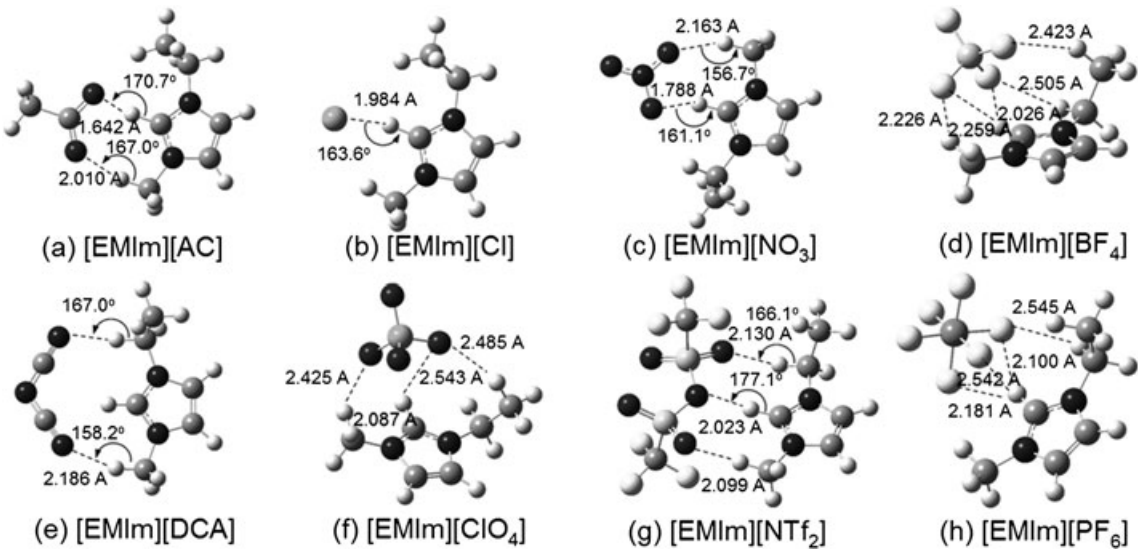

Figure 5. Optimized geometries of the nonhydroxyl ILs

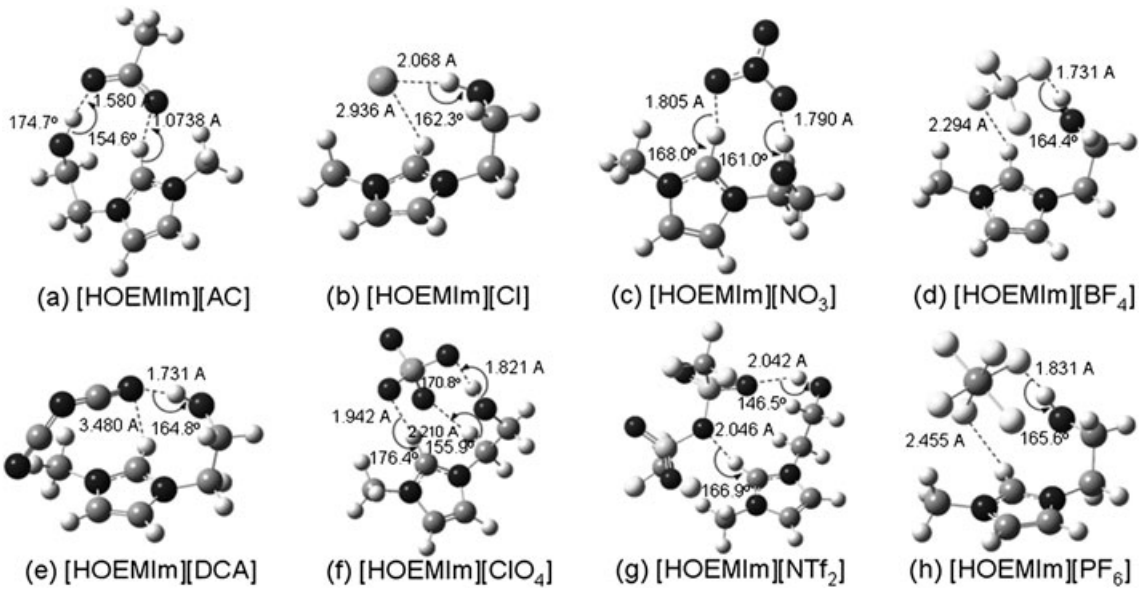

Figure 6. Optimized geometries of the hydroxyl ILs

Table 2. The calculated parameters of hydroxyl and nonhydroxyl ILs in the gas phase

ILs	ΔE_c (kcal/mol)	C2–H6 (Å)	H6···X (Å)	O–H20 (Å)	H20···X (Å)	v_a(C2–H6) (cm^{-1})	v_a(O–H20) (cm^{-1})
$[EMIm]^+$	—	1.079	—	—	—	3298	—
$[EMIm][NTf_2]$	−73.1	1.095	2.023	—	—	3059	—
$[EMIm][PF_6]$	−75.7	1.080	2.100	—	—	3289	—
$[EMIm][ClO_4]$	−78.7	1.084	2.087	—	—	3224	—
$[EMIm][BF_4]$	−81.5	1.081	2.026	—	—	3266	—
[EMIm][DCA]	−77.5	1.082	2.344	—	—	3256	—
$[EMIm][NO_3]$	−86.5	1.106	1.788	—	—	2890	—
[EMIm][Cl]	−90.5	1.123	1.984	—	—	2620	—
[EMIm][AC]	−98.2	1.136	1.642	—	—	2455	—
$[HOEMIm]^+$	—	1.079	—	0.966	—	3314	3835
$[HOEMIm][NTf_2]$	−72.0	1.090	2.046	0.972	2.042	3129	3740
$[HOEMIm][PF_6]$	−76.6	1.078	2.455	0.975	1.831	3325	3670
$[HOEMIm][ClO_4]$	−81.2	1.090	1.942	0.983	1.821	3122	3506
$[HOEMIm][BF_4]$	−83.0	1.079	2.294	0.981	1.731	3309	3559
[HOEMIm][DCA]	−82.0	1.078	3.479	0.995	1.731	3320	3264
$[HOEMIm][NO_3]$	−88.6	1.103	1.805	0.987	1.790	2920	3437
[HOEMIm][Cl]	−94.1	1.076	2.936	0.996	2.068	3335	3252
[HOEMIm][AC]	−102.8	1.111	1.738	1.015	1.580	2795	2902

106.02° ([EMIm][ClO_4]). For all hydroxyl ILs, the most stable complexes possessed similar structural characteristics to [HOEMIm][AC] where the anion is adjacent to the O–H and C2–H. Moreover, unlike nonhydroxyl ILs, the anions in hydroxyl ILs are somewhat above the imidazolium ring, moving close to the hydroxyl group. Note that for [HOEMIm][DCA], the [DCA] anions are above the imidazolium ring with one end of the nitrogen close to the acidic hydrogen of OH and no hydrogen bonding between C2–H and anions was observed, unlike most other hydroxyl ILs.

As clearly seen in Table 1, the (C2)H···X distances in all nonhydroxyl ILs are much shorter than the van der Waals distance of X···H (O···H=2.72 Å, Cl ···H=2.95 Å, F···H=2.67 Å, N···H=2.75 Å[40]) and the bond angle of C2–H···X is close to 180°, as shown in Fig. 5, implying that there are strong hydrogen bonds between the anions and C2–H. The hydrogen bonding resulted in bond lengths of C2–H in nonhydroxyl ILs that were shortened from $[AC]^-$ to $[PF_6]^-$. In hydroxyl ILs, although the C2–H distances are slightly changed as compared with those in $[HOEMIm]^+$ cation and nonhydroxyl ILs, the (C2)H···X distances in all hydroxyl ILs are clearly lengthened. Simultaneously, the O–H distance is lengthened as compared with that of $[HOEMIm]^+$, while the distance of (O)H···X is much shorter than both the distances of (C2)H···X and the van der Waals distance of X···H.[40] Instead of C2–H···X in nonhydroxyl ILs, O–H···X in hydroxyl ILs is nearly a line with angles close to 180°, obviously larger than those of C2–H···X (angles are shown in Fig. 6). The above results imply that hydrogen bonding formed preferably between the anion and C2–H in $[EMIm]^+$-based ILs and was replaced by a much stronger one between the anion and OH in $[HOEMIm]^+$-based ILs. This was further supported by the fact that the vibration frequency of C2–H in hydroxyl ILs is less influenced compared with that in $[HOEMIm]^+$ but that of O–H obviously decreased, particularly for anions of strong hydrogen-bond acceptors.

The optimized geometries for nonhydroxyl ILs are similar to the previous theoretical reports at different levels,[38,41–46] but somewhat different from the experimentally determined single-crystal X-ray structures ([EMIm][Cl],[47] $[EMIm][NO_3]$,[48] $[EMIm][PF_6]$[49], [EMIm][BF_4] and $[EMIm][NTf_2]$[50]). For example,

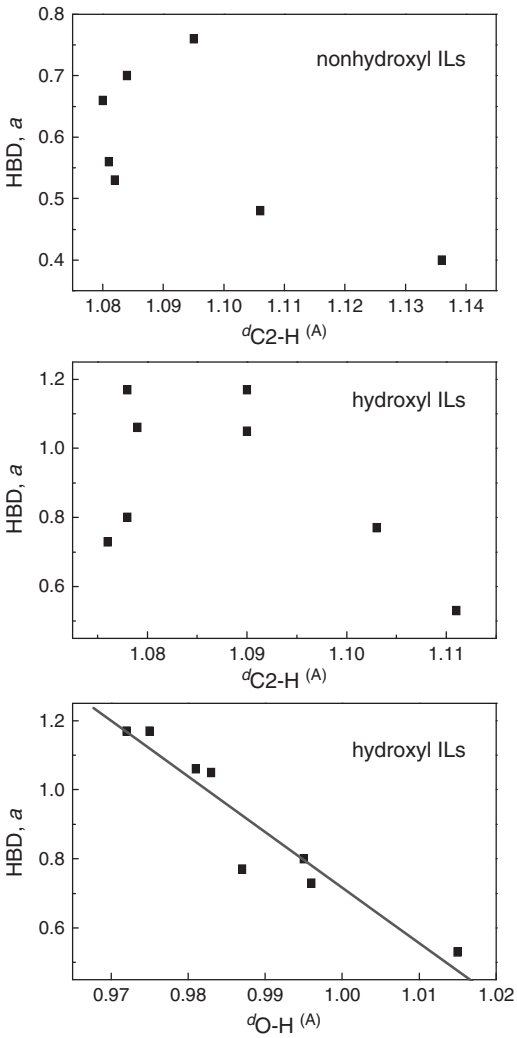

Figure 7. Plot of the HBD (*a*) versus the calculated bond length of C2–H (Å) or O–H20 (Å) for nonhydroxyl and hydroxyl ILs, respectively. The result of correlation analysis is the following: d_{O-H20}=16.82696–16.11028 *a*

Journal of Physical Organic Chemistry

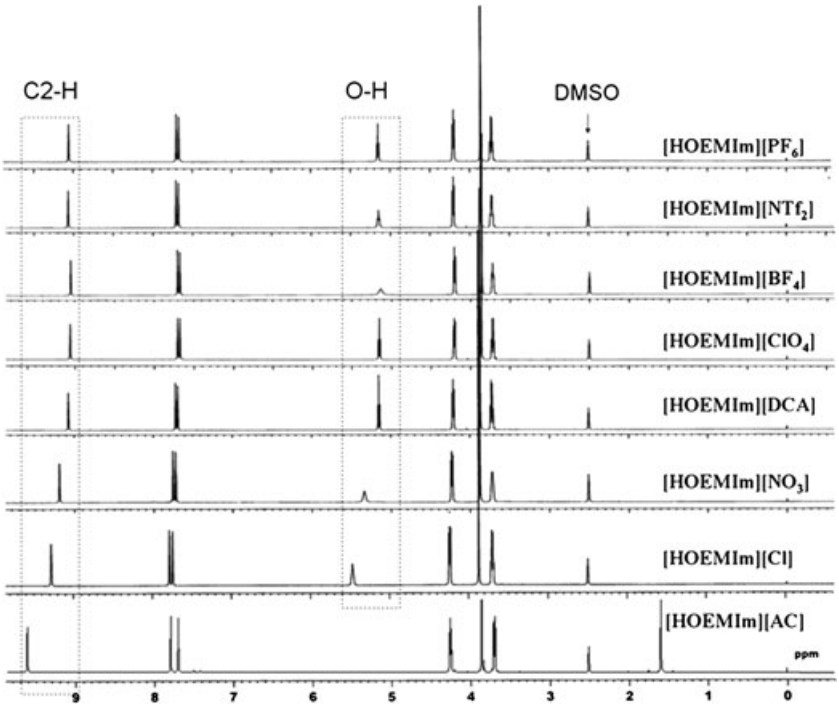

Figure 8. ^{1}H-NMR spectra of the hydroxyl ILs

Table 3. $E_T(30)$ (kcal/mol) and Kamlet–Taft Parameters (polarisability, π^*, hydrogen-bond donor acidity, α, and hydrogen-bond acceptor basicity, β) of ILs

ILs	$E_T(30)$	π^*	α	β
[EMIm][NTf_2]	52.0	0.90	0.76	0.28
[EMIm][PF_6]	52.6	0.99	0.66	0.20
[EMIm][BF_4]	53.7[a]	1.03	0.70	0.26
[EMIm][ClO_4]	52.4	1.11	0.56	0.41
[EMIm][DCA]	51.7	1.08	0.53	0.35
[EMIm][NO_3]	51.5	1.13	0.48	0.66
[EMIm][AC]	49.8	1.09	0.40	0.95
[HOEMIm][NTf_2]	60.8	1.03	1.17	0.34
[HOEMIm][PF6]	61.7[b]	1.11	1.17	0.15
[HOEMIm][BF_4][c]	60.5	1.16	1.05	0.22
[HOEMIm][ClO_4]	60.3	1.13	1.06	0.16
[HOEMIm][DCA]	56.1	1.11	0.80	0.51
[HOEMIm][NO_3]	55.6	1.11	0.77	0.65
[HOEMIm][Cl]	55.6	1.16	0.73	0.68
[HOEMIm][AC]	51.2	1.04	0.53	0.90

[a]Data from Refs. [54,56].
[b]Data from Ref. [29].
[c]Data derived from *N*,*N*-diethyl-4-nitroaniline and 4-nitroaniline.

ion packing of [EMIm][NTf_2] was reported to involve several C–H···O hydrogen bonds and C–F···F interactions, instead of C–H···N hydrogen bonds.[51] For hydroxyl ILs, there is no reasonable comparison for the properties obtained from calculated gas-phase structures with those obtained from bulk phase measurements, because of a lack of experimental data for single-crystal X-ray structures.

The magnitude of the interaction energies corrected by ZPE and BSSE for hydroxyl ILs follows the trend: $[AC]^-$>$[Cl]^-$>$[NO_3]^-$>$[BF_4]^-$>[DCA]$^-$>$[ClO_4]^-$>$[PF_6]^-$>$[NTf_2]^-$, which is nearly consistent with that of nonhydroxyl ILs. However, hydrogen bonding in ion pairing with various anions cannot be distinguished simply by ΔE_c, because the energy of the ion-pair formation is obviously larger than normal hydrogen bond energies (the hydrogen bonding energy in water dimer at the bottom of the well is only 5.0±0.1 kcal/mol[52]) and thus electrostatic attraction is the major source between ions.[53] The calculated ion-pair formation energies for hydroxyl ILs are lower than the nonhydroxyl ILs by about 0.7–4.8 kcal/mol. This implies that hydroxyls ILs are more stable than nonhydroxyl ILs. For example, ΔE_c for nonhydroxyl ILs with various anions was changed from −73.1 kcal/mol ([EMIm][NTf_2]) to −98.2 kcal/mol ([EMIm][AC]), while ΔE_c for the corresponding hydroxyl ILs was changed from −72.0 kcal/mol ([HOEMIm][NTf_2]) to −102.8 kcal/mol ([HOEMIm][AC]). Obviously, ΔE_c for [AC]-based ILs after hydroxyl functionalization only increased about 1.1 kcal/mol, while that for [NTf_2]-based ILs increased about 4.7 kcal/mol. Thus, the difference in change before and after hydroxyl functionalization can be explained, at least in part, because of the presence of positive hydrogen from OH and the formed intramolecular hydrogen bonding between anion and $[HOEMIm]^+$ (O–H···X). Together with the result of the changed trend of vibration frequency and bond length of O–H (the vibration of O–H increased from 2902 cm^{-1} for [HOEMIm][AC] to 3670 cm^{-1} for [HOEMIm][NTf_2] while its bond length shortened from 1.015 Å to 0.972 Å), the magnitude of the hydrogen bonding interaction energies in hydroxyl ILs follows the trend: $[AC]^-$>$[Cl]^-$≈[DCA]$^-$>$[NO_3]^-$>$[BF_4]^-$≈$[ClO_4]^-$>$[PF_6]^-$≈$[NTf_2]^-$.

Polarity and hydrogen bond ability of ILs

The hydrogen-bond acidity has also been explained by solvatochromism and Kamlet–Taft parameters using spectroscopic probe methods, which describe characteristics including the polarity scale, $E_T(30)$, polarisability (π^*), and hydrogen-bond

Table 4. Experimental and calculated chemical shift values of ILs with various anions[a]

Nonhydroxyl ILs[b]	C2–H		Hydroxyl ILs[b]	C2–H		OH	
	Expl	Calcd[c]		Expl	Cald[c]	Expl	Calcd[c]
[EMIm][PF_6]	9.09	10.96	[HOEMIm][PF_6]	9.06	10.03	9.09	10.96
[EMIm][NTf_2]	9.10	12.33	[HOEMIm][NTf_2]	9.07	12.01	9.10	12.33
[EMIm][BF_4]	9.09	11.15	[HOEMIm][BF_4]	9.05	10.80	9.09	11.15
[EMIm][ClO_4]	9.10	11.46	[HOEMIm][ClO_4]	9.07	12.13	9.10	11.46
[EMIm][DCA]	9.10	10.91	[HOEMIm][DCA]	9.07	9.01	9.10	10.91
[EMIm][NO_3]	9.26	15.55	[HOEMIm][NO_3]	9.19	14.50	9.26	15.55
[EMIm][Cl]	9.74[d]	17.84	[HOEMIm][Cl]	9.27	9.89	9.74[d]	17.84
[EMIm][AC]	9.81	18.49	[HOEMIm][AC]	9.61	15.57	9.81	18.49

[a]In ppm, relative to TMS.
[b]ILs in DMSO, 0.2 M.
[c]Calculated by Gaussian 03 using the B3LYP/6-31+G(d,p) method.
[d]Instead of [EMIm][Cl], [BMIm][Cl] was employed for comparison.
[e]Not observed.

donor (acidity, HBD, α) depending on the cation and hydrogen-bond acceptor (basicity, HBA, β) and on the anion properties of solvents.[54,55] As can be seen in Table 2, hydroxyl ILs exhibit more significant anion-dependent polarity ($E_T(30)$=51.2–61.7 kcal/mol) and hydrogen-bond donor acidity (α=0.53–1.17) than nonhydroxyl ILs.

According to Welton's proposition,[3] the ability of the ILs to act as a hydrogen bond donor (cation effect) is controlled and moderated by its hydrogen bond acceptor ability (anion effect), and the overall ability of the ILs to form a hydrogen bond with a solute molecule appears to come from an antagonistic relationship between its constituent ions. This may be described in terms of the following two competing equilibria.

$$[\text{Cation}]^+ + [\text{Anion}]^- \leftrightarrow [\text{Cation}]^+ \cdots [\text{Anion}]^-$$
$$[\text{Cation}]^+ + \text{Solute} \leftrightarrow [\text{Cation}]^+ \cdots \text{Solute}$$

$E_T(30)$ in nonhydroxyl imidazolium-based ILs is mainly influenced by the strength of hydrogen bonds between the phenoxide group on Reichardt's dye and the hydrogen atoms C2–H.[56] The C2–H on the imidazolium ring interact with anions of variable hydrogen bond abilities (from [AC] to [PF_6]), however, giving residual hydrogen (C2–H) comparable freedom and acidity to interact with the phenoxide group because of its lower acidity. For hydroxyl ILs, the polarity scale was mainly influenced by the more acidic OH in hydroxyl ILs, which behaves as a better hydrogen bond donor than C2–H.[30,57] The more active OH is expected to differentiate the anions of variable hydrogen bond ability through hydrogen bonding between OH and anions, giving hydrogen different freedom and acidity to interact with the solute. For example, the acidic OH in [HOEMIm][AC] is anchored by the enhanced hydrogen bonding interaction between OH and $[AC]^-$, which is much stronger than that in [HOEMIm][PF_6], leading to a weak interaction with the probe molecule.

A plot of the HBD (*a*) versus the calculated bond length of C2–H (Å) and O–H20 (Å) for nonhydroxyl and hydroxyl ILs, respectively, is shown in Fig. 7. Obviously, *a* value monotonously decreased with the increasing bond length of O–H20 when varying the anion from [AC] to [NTf_2], with good linearity (R=0.95). However, no obvious correlation between bond length of C2–H and *a* value was obtained either in hydroxyl ILs or in nonhydroxyl ILs. The result supported the fact that the HBD ability of hydroxyl ILs is mainly exhibited by the much more acidic hydrogen on OH rather than by C2–H and for nonhydroxyl ILs, the effect of anions on the HBD ability exhibited by C2–H is not pronounced.

^{1}H-NMR

The calculated results are further compared with the experimental results of ^{1}H-NMR, taking into consideration the fact that ion pairing occurs preferentially between the acidic hydrogen of the cations and counter ions and the ^{1}H-NMR properties of ILs are also revealed as highly dependent on the nature of the anion and the interaction between cation and anion.[58,59]

The ^{1}H-NMR results for the ILs diluted in DMSO-d_6 at identical concentrations are given in Fig. 8 and the chemical shift of protons on C2 and OH in hydroxyl and nonhydroxyl ILs with different anions are listed in Table 3. For all hydroxyl ILs, the chemical shift of methylene and methyl hydrogen is generally anion-independent, while the chemical shift of C4/C5–H slightly increased with anion basicity, which may be because of the hydrogen-bonded network between cations and anions in ILs,[19] but not ring stacking, because the former leads to a higher chemical shift while the latter leads to a lower chemical shift.[60]

In contrast, the chemical shift of C2–H significantly increased with anion basicity, consistent with an earlier work by Bonhote *et al.*[60] For hydroxyl ILs with weak hydrogen-bond acceptors such as the anions $[PF_6]^-$, $[NTf_2]^-$, and $[ClO_4]^-$, the chemical shift of C2–H was nearly constant after hydroxyl function, which means that the anions are too inert to interact with OH and to disturb the interaction between C2–H and the anions. However, for hydroxyl ILs with the anions $[NO_3]^-$, $[Cl]^-$, and $[AC]^-$, one can see that the chemical shift of C2–H significantly decreased (moved to a higher field) compared with nonhydroxyl ILs. This is caused by the competing formation of strong hydrogen bonding between OH and the basic anion, which gives rise to relatively free C2–H that is less intimated with the anion. Simultaneously, the higher-field chemical shift of OH from 5.15 for [HOEMIm][PF_6] to 5.48 for [HOEMIm][Cl] further supported this point. This OH···X hydrogen bonding-induced change of chemical shift of C2–H was also observed in equimolar mixtures

of [BMIm][Br] and diol compounds.[61] After hydroxyl functionization, the unexpected slight change of chemical shift of C2–H in $[AC]^-$-based ILs is indicative of a small change in the hydrogen bond of C2–H···$[AC]^-$, probably because of the presence of two equivalent electro-negative oxygens on the anion.

^{1}H-NMR chemical shifts of nonhydroxyl and hydroxyl ILs was also obtained by DFT calculations. As shown in Table 4, although the calculated chemical shifts of C2–H and OH of the ion pair optimized in the gas phase are significantly more deshielded than the experimental data, the change in trend of the chemical shifts are roughly consistent with that of the experimental results, which confirmed the anion-dependent hydrogen bonding in hydroxyl ILs. It is noteworthy that the calculated chemical shifts of C2–H in [HOEMIm][Cl] and [HOEMIm][DCA] are much lower than those in other hydroxyl ILs, which could be a result of their nonplanar conformations (where anions are on the imidazolium ring), similar to the calculated result of two different [EMIm][Cl] conformations as reported by Bagno *et al*.[62]

CONCLUSIONS

In summary, in $[EMIm]^+$-based nonhydroxyl ILs, hydrogen bonding is mainly between anions and C2–H (C2–H···X). However, in $[HOEMIm]^+$-based hydroxyl ILs, the presence of OH make it a better hydrogen bond donor than C2–H. Strong hydrogen bonding interaction occurred between anions and OH on the cation (O–H···X). The resulting hydrogen bonding is much more anion-dependent than the C2–H···anion, where it is obviously weakened by changing the anion from $[AC]^-$ to $[NTf_2]^-$. This different interaction between $[HOEMIm]^+$ and variable anions involving O–H···X hydrogen bonding resulted in the hydrogen of OH with different acidity and freedom to interact with the probe molecule, thus the anion in hydroxyl ILs exhibited a significant effect on their bulk phase properties. Experimental results of hydroxyl ILs indeed show anion-dependent polarity and HBD (acidity, α), and ^{1}H-NMR shift, more significantly than nonhydroxyl ILs.

Acknowledgement

This work was supported by the National Natural Science Foundation of China (No. 20533080). The authors thank the supercomputing center, Computer Network Information Center (CNIC), Chinese Academy of Sciences (CAS) for Gaussian calculations.

REFERENCES

[1] P. Wasserscheid, W. Keim, *Angew. Chem. Int. Ed.* **2000**, *39*, 3772.
[2] T. Welton, *Chem. Rev.* **1999**, *99*, 2071.
[3] P. Wasserscheid, T. Welton, *Ionic liquids in synthesis* Vol. *2*, Wiley-VCH, Weinheim, Germany, **2007**.
[4] N. V. Plechkova, K. R. Seddon, *Chem. Soc. Rev.* **2008**, *37*, 123.
[5] T. L. Merrigan, E. D. Bates, S. C. Dorman, J. H. Davis, *Chem. Commun.* **2000**, 2051.
[6] D. R. MacFarlane, J. Golding, S. Forsyth, M. Forsyth, G. B. Deacon, *Chem. Commun.* **2001**, 1430.
[7] H. Tokuda, S. Tsuzuki, M. A. B. H. Susan, K. Hayamizu, M. Watanabe, *J. Phys. Chem. B* **2006**, *110*, 19593.
[8] M. Smiglak, A. Metlen, R. D. Rogers, *Acc. Chem. Res.* **2007**, *40*, 1182.
[9] M. C. Tseng, Y. H. Chu, *Chem. Commun.* **2010**, *46*, 2983.
[10] P. Wang, S. M. Zakeeruddin, I. Exnar, M. Gratzel, *Chem. Commun.* **2002**, 2972.
[11] R. P. Singh, R. D. Verma, D. T. Meshri, J. M. Shreeve, *Angew. Chem. Int. Ed.* **2006**, *45*, 3584.
[12] F. Zhou, Y. M. Liang, W. M. Liu, *Chem. Soc. Rev.* **2009**, *28*, 2590.
[13] S. Millefiorini, A. H. Tkaczyk, R. Sedev, J. Efthimiadis, J. Ralston, *J. Am. Chem. Soc.* **2006**, *128*, 3098.
[14] W. Xu, E. I. Cooper, C. A. Angell, *J. Phys. Chem. B* **2003**, *107*, 6170.
[15] Z. Fei, D. R. Zhu, X. Yang, L. Meng, Q. Lu, W. H. Ang, R. Scopelliti, C. G. Hartinger, P. J. Dyson, *Chem. Eur. J.* **2010**, *16*, 6473.
[16] P. Kolle, R. Dronskowski, *Inorg. Chem.* **2004**, *43*, 2803.
[17] A. Wulf, K. Fumino, R. Ludwig, *Angew. Chem. Int. Ed.* **2010**, *49*, 449.
[18] R. C. Remsing, J. L. Wildin, A. L. Rapp, G. Moyna, *J. Phys. Chem. B* **2007**, *111*, 11619.
[19] K. Dong, S. J. Zhang, D. X. Wang, X. Q. Yao, *J. Phys. Chem. A* **2006**, *110*, 9775.
[20] K. Fumino, A. Wulf, R. Ludwig, *Angew. Chem. Int. Ed.* **2008**, *47*, 3830.
[21] H. Ohno, Y. Fukaya, *Chem. Lett.* **2009**, *38*, 2.
[22] S. Wallert, K. Drauz, I. Grayson, H. Groger, P. D. D. Maria, C. Bolm, *Green Chem.* **2005**, *7*, 602.
[23] S. V. Dzyuba, R. A. Bartsch, *Tetrahedron Lett.* **2002**, *43*, 4657.
[24] L. Ren, L. Meng, Q. Lu, *Chem. Lett.* **2008**, *37*, 106.
[25] X. Yang, N. Yan, Z. F. Fei, R. M. Crespo-Quesada, G. Laurenczy, L. Kiwi-Minsker, Y. Kou, Y. D. Li, P. J. Dyson, *Inorg. Chem.* **2008**, *47*, 7444.
[26] X. Wei, L. Yu, D. Wang, X. Jin, G. Z. Chen, *Green Chem.* **2008**, *10*, 296.
[27] X. Wei, L. Yu, X. Jin, D. Wang, G. Z. Chen, *Adv. Mater.* **2009**, *21*, 776.
[28] Y. Wu, T. Sasaki, K. Kazushi, T. Seo, K. Sakurai, *J. Phys. Chem. B* **2008**, *112*, 7530.
[29] S. Zhang, Q. Zhang, B. Ye, X. Li, X. Zhang, Y. Deng, *J. Phys. Chem. B* **2009**, *113*, 6012.
[30] S. G. Zhang, X. J. Qi, X. Y. Ma, L. J. Lu, Y. Q. Deng, *J. Phys. Chem. B* **2010**, *114*, 3912.
[31] M. J. Frisch, G. W. Trucks, H. B. Schlegel, G. E. Scuseria, M. A. Robb, J. R. Cheeseman, J. A. Montgomery, Jr., T. Vreven, K. Kudin, J. C. N. Burant, J. M. Millam, S. S. Iyengar, J. Tomasi, V. Barone, B. Mennucci, M. Cossi, G. Scalmani, N. Rega, G. A. Petersson, H. Nakatsuji, M. Hada, M. Ehara, K. Toyota, R. Fukuda, J. Hasegawa, M. Ishida, T. Nakajima, Y. Honda, O. Kitao, H. Nakai, M. Klene, X. Li, J. E. Knox, H. P. Hratchian, J. B. Cross, C. Adamo, J. Jaramillo, R. Gomperts, R. E. Stratmann, O. Yazyev, A. J. Austin, R. Cammi, C. Pomelli, J. W. Ochterski, P. Y. Ayala, K. Morokuma, G. A. Voth, P. Salvador, J. J. Dannenberg, V. G. Zakrzewski, S. Dapprich, A. D. Daniels, M. C. Strain, O. Farkas, D. K. Malick, A. D. Rabuck, K. Raghavachari, J. B. Foresman, J. V. Ortiz, Q. Cui, A. G. Baboul, S. Clifford, J. Cioslowski, B. B. Stefanov, G. Liu, A. Liashenko, P. Piskorz, I. Komaromi, R. L. Martin, D. J. Fox, T. Keith, M. A. Al-Laham, C. Y. Peng, A. Nanayakkara, M. Challacombe, P. M. W. Gill, B. Johnson, W. Chen, M. W. Wong, C. Gonzalez, J. A. Pople, Gaussian 03, revision E.01, Gaussian, Inc.: Pittsburgh, PA, **2003**.
[32] E. A. Turner, C. C. Pye, R. D. Singer, *J. Phys. Chem. A* **2003**, *107*, 2277.
[33] S. F. Boys, F. Bernardi, *Mol. Phys.* **1970**, *19*, 553.
[34] Y. Fu, L. Liu, R. C. Li, R. Liu, Q. X. Guo, *J. Am. Chem. Soc.* **2004**, *126*, 814.
[35] Z. X. Mou, P. Li, Y. X. Bu, W. H. Wang, J. Y. Shi, R. Song, *J. Phys. Chem. B* **2008**, *112*, 5088.
[36] J. S. Murray, P. Politzer, *J. Mol. Struct. Theochem* **1998**, *425*, 107.
[37] P. Politzer, J. S. Murray, Z. Peralta-Inga, *Int. J. Quantum Chem* **2001**, *85*, 676.
[38] Y. Wu, T. Zhang, *J. Phys. Chem. A* **2009**, *113*, 12995.
[39] L. He, G. H. Tao, D. A. Parrish, J. M. Shreeve, *J. Phys. Chem. B* **2009**, *113*, 15162.
[40] A. Bondi, *J. Phys. Chem.* **1964**, *68*, 441.
[41] S. A. Katsyuba, P. J. Dyson, E. E. Vandyukova, A. V. Chernova, A. Vidis, *Helv. Chim. Acta* **2004**, *87*, 2556.
[42] N. Sun, X. Z. He, K. Dong, X. P. Zhang, X. M. Lu, H. Y. He, S. J. Zhang, *Fluid Phase Equilib.* **2006**, *246*, 137.
[43] N. E. Heimer, R. E. Del Sesto, Z. Z. Meng, J. S. Wilkes, W. R. Carper, *J. Mol. Liq.* **2006**, *124*, 84.
[44] V. N. Emel'yanenko, S. P. Verevkin, A. Heintz, C. Schick, *J. Phys. Chem. B* **2008**, *112*, 8095.
[45] N. Akai, D. Parazs, A. Kawai, K. Shibuya, *J. Phys. Chem. B* **2009**, *113*, 4756.
[46] V. N. Emel'yanenko, S. P. Verevkin, A. Heintz, *J. Am. Chem. Soc.* **2007**, *129*, 3930.
[47] C. J. Dymek, D. A. Grossie, A. V. Fratini, W. W. Adams, *J. Mol. Struct.* **1989**, *213*, 25.
[48] J. S. Wilkes, M. J. Zaworotko, *J. Chem. Soc., Chem. Comm.* **1992**, 965.
[49] J. Fuller, R. T. Carlin, H. C. Delong, D. Haworth, *J. Chem. Soc., Chem. Comm.* **1994**, 299.
[50] The molecular structures of the very low.
[51] A. R. Choudhury, N. Winterton, A. Steiner, A. I. Cooper, K. A. Johnson, *CrystEngComm* **2006**, *8*, 742.

[52] M. W. Feyereisen, D. Feller, D. A. Dixon, *J. Phys. Chem.* **1996**, *100*, 2993.
[53] S. Tsuzuki, H. Tokuda, K. Hayamizu, M. Watanabe, *J. Phys. Chem. B* **2005**, *109*, 16474.
[54] C. Reichardt, *Green Chem.* **2005**, *7*, 339.
[55] L. Crowhurst, P. R. Mawdsley, J. M. Perez-Arlandis, P. A. Salter, T. Welton, *Phys. Chem. Chem. Phys.* **2003**, *5*, 2790.
[56] M. J. Muldoon, C. M. Gordon, I. R. Dunkin, *J. Chem. Soc., Perk. Trans. 2* **2001**, 433.
[57] A. Paul, A. Samanta, *J. Phys. Chem. B* **2007**, *111*, 4724.
[58] L. I. N. Tome, F. R. Varanda, M. G. Freire, I. M. Marrucho, J. A. P. Coutinho, *J. Phys. Chem. B* **2009**, *113*, 2815.
[59] J. Palomar, V. R. Ferro, M. A. Gilarranz, J. J. Rodriguez, *J. Phys. Chem. B* **2007**, *111*, 168.
[60] P. Bonhote, A. P. Dias, N. Papageorgiou, K. Kalyanasundaram, M. Gratzel, *Inorg. Chem.* **1996**, *35*, 1168.
[61] H. Shimura, M. Yoshio, K. Hoshino, T. Mukai, H. Ohno, T. Kato, *J. Am. Chem. Soc.* **2008**, *130*, 1759.
[62] A. Bagno, F. D'Amico, G. Saielli, *Chemphyschem* **2007**, *8*, 873.